Letters in Applied NanoBioScience
Open-Access Journal (ISSN: 2284-6808)

Article
Volume 13, Issue 4, 2024, 159
https://doi.org/10.33263/LIANBS134.159

Molecular Docking and Dynamics of *Syzygium aromaticum* as Antidiabetic Potential Drugs Targeting Alpha-Glucosidase and Alpha-Amylase

Fernanda Chairunisa [1], Riyan Alifbi Putera Irsal [2]

[1] Universitas Nasional, Pasar Minggu, South Jakarta, Indonesia
[2] Biomatics, Bogor, West Java, Indonesia
* Correspondence: fernandachairunisa@civitas.unas.ac.id;

Scopus Author ID 58932764900
Received: 27.10.2023; Accepted: 12.05.2024; Published: 25.08.2024

Abstract: 86% of the 17 million people who die from degenerative diseases are from middle and low-income countries, one of which is Indonesia. Four main diseases cause degenerative diseases, and one of them is diabetes. Diabetes treatment generally uses chemical drugs that have long-term side effects. Therefore, the use of natural-based herbal medicines for treating diabetes is needed, one of which is clove (*Syzygium aromaticum*), a typical Indonesian plant that has been trusted as traditional medicine. This study aimed to determine compounds from cloves that effectively inhibit alpha-amylase and alpha-glucosidase enzymes as antidiabetic drug candidates. The determination was made using molecular docking and dynamics simulations. This study used the enzymes alpha-amylase (1B2Y) and alpha-glucosidase (2QMJ) as receptors, acarbose as natural ligands, and active compounds from cloves. The best inhibition of both enzymes is owned by stigmasterol ligands with binding free energy of -9506 cal/mol to alpha-amylase and -8385 cal/mol to alpha-glucosidase. The average free binding energy of stigmasterol-3-O-beta-D-glucopyranoside ligands is better than natural ligands from both alpha-glucosidase and alpha-amylase based on the best results from molecular dynamics simulations with values of 2327 cal/mol and 27374 cal/mol.

Keywords: binding energies; diabetic; herbal medicine; Yasara structure.

1. Introduction

Non-communicable diseases or degenerative diseases are defined as a premature decline in cell function, which provokes the emergence of various diseases. 86% of the 17 million people who die from degenerative diseases are from middle and low-income countries [1]. Degenerative diseases in the future are projected to increase, especially for populations affected by humanitarian crises and natural disasters that cause increased mortality and morbidity [2,3]. There are four main diseases that cause degenerative diseases such as cancer, chronic respiratory diseases, coronary heart disease, and diabetes [1]. Diabetes is one of the diseases that become a huge health problem in Indonesia and also the world. The total comparative prevalence of diabetes at the age of 20 – 79 years reaches 10.6% of the global population in 2021 and is predicted to increase by 0.7% in 2030 [4]. Indonesia has a comparative prevalence of diabetes at the age of 20 – 79 years, as much as 10.6% of the total population in 2021, and is expected to continue to increase, considering that Indonesia is a lower-middle-income country [4,5].

Diabetes or diabetes mellitus (DM) is a metabolic disease characterized by increased blood glucose levels. Diabetes is a challenge for the world, especially in global health problems, because it can trigger the emergence of vascular complications such as CHD, which makes diabetes a primary risk factor for vascular complications [6]. Diabetes itself is divided into two types, diabetes type 1 and type 2, with type 1 sufferers having a lower life expectancy due to their involvement with complications of cardiovascular disease and acute metabolic disorders [7]. Research [8] states that the harmony between diabetes and CHD occurs due to several risk factors, such as unhealthy lifestyles and smoking habits, based on the results of data analysis of the US National Health and Nutrition Examination Survey. Treatment of diabetes and its complications generally uses chemical drugs that have long-term side effects. Therefore, the use of natural-based herbal medicines for treating diabetes is needed, especially for preventing complications, one of which is clove, a typical Indonesian plant that has been trusted as traditional medicine in Indonesia [9].

Cloves (*Syzygium aromaticum*) are known as dried bud flowers of the Myrtaceae family, originating from the Maluku Islands of Indonesia. Cloves contain various bioactive compounds, and phenolic compounds are the most widely identified compounds in cloves, especially volatile compounds such as eugenol [10]. Cloves attract the world's attention because of their benefits, which can be used for commercial purposes, so many countries are trying to cultivate them. Cloves provide a large share in the pharmaceutical industry, perfumes, beauty, and food, and also as a valuable spice. The role of cloves in inhibiting degenerative diseases is excellent because they can be an antioxidant in the cellular system to increase cell viability due to oxidative stress significantly from clove extract [11]. Research related to the benefits of cloves has been widely carried out. Still, there has been no research related to the search for antidiabetic drugs that directly target the key enzymes that cause diabetes, alpha-amylase and alpha-glucosidase.

Based on this background, this study aimed to determine compounds from cloves (Syzygium aromaticum) that effectively inhibit alpha-amylase and alpha-glucosidase enzymes as antidiabetic drug candidates. The determination was made through molecular docking simulation methods, followed by a look at its stability through molecular dynamics simulations. This study is useful to provide information to researchers in the form of molecular and stability of the interaction of receptor-ligand active compounds of cloves on the target enzyme that causes diabetes, which can be used as an initial reference for making potential inhibitors and as a candidate for antidiabetic drugs made from natural ingredients typical of Indonesia.

2. Materials and Methods

2.1. Materials.

The equipment used is in the form of personal computer hardware with AMD Ryzen 5 3600 specifications with NVIDIA GeForce RTX 3060, Windows 11 operating system, and YASARA software version 19.9.17 Discovery Studio 2017, notepad++, and Pymol.org. The materials used were the PDB ligand *Syzygium aromaticum*, as many as 43 ligands obtained from literature studies in several journals (Table 1), and two enzymes, namely alpha-glucosidase (PDB ID: 2QMJ) and alpha-amylase (PDB ID: 1B2Y).

Table 1. Constituents of *Syzygium aromaticum.*

No	Constituents	CID	Literature
1	Eugenol	3314	[12]
2	beta-caryophelline	5281515	[12]
3	aeruginosin	71463188	[12]
4	quercetin	5280343	[12]
5	euparin	119039	[12]
6	L-Noradrenaline	439260	[12]
7	benzofura	102437377	[12]
8	gallic acid	370	[12]
9	Myricetin	5281672	[13, 14]
10	2-Heptanone	8051	[13, 14]
11	5-Hydroxytryptamine	5202	[13]
12	Tryptamine	1150	[13]
13	Biflorin	441959	[13, 14]
14	Syringic acid	10742	[13]
15	Vanillin	1183	[13, 14]
16	Casuarictin	73644	[13, 14]
17	Eugeniin	442679	[13]
18	Tellimagrandin I	442690	[13, 14]
19	Campesterol	173183	[13]
20	Kaempferol	5280863	[13, 14]
21	Rhamnocitrin	5320946	[13]
22	Rhamnetin	5281691	[13, 14]
23	Isoengeletin	101937309	[13]
24	Ellagic acid	5281855	[13, 14]
25	Viscic acid	38348725	[13]
26	Oleanolic acid	10494	[13, 14]
27	3-O-beta-D-Glucopyranosyl sitosterol	70699351	[13]
28	Stigmasterol-3-O-beta-D-glucopyranoside	6602508	[13, 14]
29	Eugenin	10189	[13, 14]
30	Isobiflorin	85114699	[13]
31	Methyl salicylate	4133	[13, 14]
32	Strictinin	73330	[13, 14]
33	Isoeugenitin	12310980	[13, 14]
34	Isoeugenitol	5318562	[13, 14]
35	m-Methoxybenzaldehyde	11569	[13, 14]
36	5-Methoxytryptamine	1833	[13]
37	Melatonin	896	[13]
38	Aceteugenol	7136	[13]
39	2-Acetyl-4-beta-D-glucopyranosyl-1,3,5-benzenetriol.	10892862	[13]
40	Syzyginin A	102445429	[13]
41	Syzyginin B	102445430	[13]
42	Daucosterol	5742590	[14]
43	Tellimagrandin 2	151590	[14]

2.2. Procedures.

2.2.1. Preparation of constituents and enzymes obtained.

The 3D structure of the receptor is downloaded from the RCSB Protein Data Bank on the www.rcsb.org/pdb/ page with PDB codes 1B2Y and 2QMJ. The 3D structure of the receptor was prepared, and the natural ligand was separated from the receptor in the Yasara Structure. The 3D structure of the test and comparison ligands can be downloaded at https://www.pubchem.ncbi.nlm.nih.gov [15].

2.2.2. Validation grid box of enzymes.

The size and location of the grid box are adjusted to the active site of the receptors or ligands tethered to PDB with a grid box size range of 1 Å to 5 Å with an interval of 0.5 Å. Method validation (grid box) is acceptable if the RMSD value obtained is < 2.0 Å. The first

docking simulation was carried out to validate the grid box by means of natural ligand redocking. Running docking can be processed by opening the dock_run.mcr file and the docking process is carried out 100 times. Docking results can be read in the .log file [16].

2.2.3. Virtual screening of *Syzygium aromaticum* against enzyme targets.

The best grid box with the largest (positive) binding energy and RMSD < 2.0 Å validation results are used for virtual screening. Running docking can be processed by opening the file dock_runscreening.mcr, and the docking process is carried out 10 times. Results can be read in a .txt file. Visualization/analysis related to types of interactions between ligand-receptors, such as hydrogen bonds and hydrophobic interactions, in two dimensions using Discovery Studio 2017. Analysis/visualization of molecular interactions in three dimensions using PyMol [15].

2.2.4. ADMET properties of *Syzygium aromaticum.*

Toxicity prediction is done on the page http://lmmd.ecust.edu.cn/admetsar1/predict/ in SMILES format, which is admetSAR 1.0 software. The results of the analysis were hERG inhibition, carcinogenicity, and acute oral toxicity [17].

2.3. Molecular dynamics simulation.

The docked PDB file is opened in YASARA-Structure. The MD simulation is run using the "md_run.mcr" macro with modifications to a duration of 100 ns. The physical conditions of the simulated cells were set at 300K, pH 7.4, and 0.9% NaCl. After the simulation is complete, the MD simulation is continued on the ligand complex. The MD simulation path analysis was analyzed using the default "md_analyze.mcr" and "md_analyzebindenergy.mcr" macro from YASARA-Structure to calculate Root Mean Square Deviation (RMSD), radius of gyration, Root Mean Square Fluctuation (RMSF), and Molecular Mechanics Poisson–Boltzmann Surface Area (MM-PBSA). Microsoft Excel is used for quantitative analysis of simulation results and tidying up data displayed in graphical form (modified from [17]).

3. Results and Discussion

3.1. Validation grid box of enzymes.

Grid box validation is used to get the best grid box covering the active site of the enzyme. The results of Table 2 show that the best grid box for the alpha-glucosidase enzyme is 4.5 Å, while the grid box for alpha-amylase is 3.0 Å. grid box size 4.5 produces binding energy and RMSD (Root Mean Square Deviation) of 7,959 kcal/mol and 1,499 Å. Grid box 3.0 A produces binding energy and RMSD of 9,742 kcal/mol and 0,744 Å. A good grid box has valid parameters of the grid box molecular docking method, which has an RMSD value of ≤ 2 Å. The RMSD value is expressed as good when the RMSD value ≤ 2.0 Å, which interprets that the orientation of the crystallographic binding on the active side of the protein with the same ligand is bound to the right position [18]. Therefore, the validation results on both enzymes are good or bound to the right position.

Table 2. Validation grid box of enzymes.

No	*Grid box* (Å)	Alpha-glucosidase		Alpha amylase	
		ΔG (kcal/mol)	RMSD(Å)	ΔG (kcal/mol)	RMSD(Å)
1	0.5	7,801	1,567	9,685	0.801
2	1.0	7,790	1,584	9,659	0.761

No	*Grid box* (Å)	Alpha-glucosidase		Alpha amylase	
		ΔG (kcal/mol)	RMSD(Å)	ΔG (kcal/mol)	RMSD(Å)
3	1.5	7,771	1,644	9,552	0.886
4	2.0	7,802	1,553	9,678	0.794
5	2.5	7,789	1,562	9,659	0.769
6	3.0	7,779	1,555	9,742	0.744
7	3.5	7,781	1,621	9,652	0.842
8	4.0	7,781	1,559	9,639	0.775
9	4.5	7,959	1,499	-0.94	4.678
10	5.0	7,087	1,574	9,667	0.775
11	5.5	7,787	1,576	9,542	0.748
12	6.0	7,788	1,585	9.443	0.790

Desc: Green box = the best grid box.

3.2. Virtual screening of Syzygium aromaticum against enzyme targets.

Alpha-glucosidase (PDB: 2QMJ) and alpha-amylase (PDB: 1B2Y) have their own active site that activates the action of the enzymes. Active site of alpha glucosidase are ASP443 and GLU446. The active sites of alpha-amylase are ASP197 and GLU233. We report that *Syzygium aromaticum* has the potential to be an inhibitor of alpha-glucosidase (Table 3) and alpha-amylase (Table 4). The molecular interaction of the best constituent with alpha-glucosidase is shown in Figure 1. Meanwhile, molecular interaction with alpha-amylase is shown in Figure 1.

Table 3. Virtual screening of alpha-glucosidase.

Constituents	Alpha-glucosidase 2QMJ				
	ΔG (cal/mol)	Ki (µM)	Interaction		
			Hydrogen bond	Hydrophobic bond	Van der Walls
Acarbose (control drug)	-7805	1.915	His600, Asp327, Thr205	Phe575, Tyr299	Ile364, Trp441, Arg598, Trp539, Arg526, Met444, Phe450, Leu577, Ala576, Thr544, Asn207, Thr204, Trp406, Ile328
Stigmasterol-3-O-beta-D-glucopyranoside	-8385	0.720	Thr544	Met444, Phe575, His600, Tyr299, Ile328, Trp406, Ala576	Leu577, Thr546, Gly208, Asp549, Asn207, Thr205, Tyr605, Phe450, Asp203, Arg526, Asp443, Trp539, Trp441, Ile364, Asp327, Asp542
3-O-beta-D-Glucopyranosylsitosterol	-8226	0.941	Asp549	Met444, Trp406, Tyr299, Ile328, Phe575, Ala576	Asp203, Phe450, Asp542, Arg526, Trp441, His600, Trp539, Asp443, Asp327, Ile364, Tyr605, Thr205, Thr544, Asn207, Trp552, Gly208, Thr546, Leu577
Daucosterol	-8226	0.941	Asp549	Ala576, Ile328, Phe575, Tyr299, Met444, Trp406	Phe450, Asp203, Leu577, Thr546, Gly208, Trp552, Asn207, Thr544, Thr205, Tyr605, Ile364, Asp327, Asp443, Trp539, His600, Trp441, Arg526, Asp542, Phe450, Asp203
Strictinin	-8219	0.953	Arg202, Asp203	Lys480, Phe575	Asp474, Thr204, Phe450, Met444, Trp406, Arg526, Asp542, Trp539, Trp441, His600, Ile364, Asp327, Ile328, Tyr299
Aeruginosin	-8069	1.227	Thr205, Thr544, Asp327, Asp542	Ala576, Trp406, Tyr299, Phe575, Ile328, Trp441, His600, Trp539	Asn543, Tyr605, Lys480, Asn449, Ser448, Met444, Tyr214, Thr204, Arg202, Arg526, Ile364
Casuarictin	-7987	1.409	Asp327, Arg526, Phe450, Thr205, Asp203, Lys480	Phe575,	Ile364, Trp441, Trp539, Tyr299, His600, Asp542, Gly602, Ile328, Met444, Trp406, Phe450, Arg202,
Benzofura	-7831	1.833	-	Phe575, Trp406, Phe450	Asp203, Thr204, Thr205, Asp542, Tyr214, Ala576, Arg526, Tyr299, Asp443, Asp327, Met444, Lys480
Myrecetin	-7653	2.475	Asp203, Tyr299, Asp327	Trp406, Phe575	Ser448, Phe450, Ile328, Ile364, His600, Trp441, Trp539, Arg526

Constituents	Alpha-glucosidase 2QMJ				
	ΔG (cal/mol)	Ki (μM)	Interaction		
			Hydrogen bond	Hydrophobic bond	Van der Walls
Syzyginin A	-7638	2.538	Asn449, Phe450, Lys480, Asp474, Thr204, Asn207	Leu473, Ala576	Ser448, Asp203, Tyr605, Phe575, Met444, Tyr299, Trp406, Arg526, Ser448, Thr211, Asn209, Thr205, Thr544

Table 4. Virtual screening of alpha-amylase.

Constituents	Alpha-amylase (1B2Y)				
	ΔG (cal/mol)	Ki (μM)	Interaction		
			Hydrogen bond	Hydrophobic bond	Van der Walls
Acarbose (control drug)	-9735	0.074	Gln63, Trp59, His101, His201, Lys200	Leu165	Gly306, Arg195, His299, Trp58, Ala307, Tyr151, Ile235, Leu162, Ala198,Tyr62, Val98, His101, Glu60, Gln63, Gly104, Gly164
Stigmasterol-3-O-beta-D-glucopyranoside	-9506	0.109	Glu240, Lys200	His305, Trp59, Leu165, Leu162, His101	Gln63, Tyr62, His201, Tyr151, Leu237, Ala307, Gly308, Ile235, Gly306, Glu233, Asp300, Thr163, Trp58
Campesterol	-9438	0.122	His201	Trp59, Ile235, Ala198, Leu162	Tyr62, Leu165, Trp58, Asp300, His101, Glu233, Gly306, Lys200, Tyr151, Thr163, His305, Gln63
Oleanolic acid	-9352	0.141	Tyr151	Leu162, Trp59, Ile235, Leu165	Thr163, Gln63, Tyr62, Trp58, His305, Asp300, Gly306, Ala307, His201, Lys200
3-O-beta-D-Glucopyranosylsitosterol	-9266	0.163	Lys200, Glu240, Gly306	Leu165, His101, Leu162, His305, Trp59	Gln63, Tyr62, His201, Gly308, Ala307, Leu237, Ile235, Tyr151, Asp300, Glu233, Thr163, Trp58
Deucasterol	-9196	0.183	Gly306, Glu240, Lys200	Leu165, His101, Leu162, Trp59, His305	Gln63, Tyr62, His201, Gly308, Ala307, Leu237, Ile235, Tyr151, Glu233, Asp300, Thr163, Trp58
Myricetin	-9175	0.190	Asp197, Tyr62, Gln63	Trp59	His305, Leu162, Ala198, Glu233, Arg185, Asp300, His299, Trp58, Leu165, His101
Quercetin	-8976	0.266	Asp300, His299, Asp197, Glu233, Tyr62, Gln63	Trp59	His305, Trp58, Arg195, Ala198, Leu162, Leu165, His101
Rhamnetin	-8976	0.266	Asp300, Tyr62, Glu233	Trp59	Leu162, Leu165, Thr163, Ala198, Asp197, Arg195, His299, Trp58, His305
Benzofura	-8955	0.275	Gly306, His305, Gln63	Leu165	Ala198, Glu233, Leu162, Asp300, Tyr151, Ile235, His201, Asp356, Gly304, Asn352, Thr163, Tyr62

3.3. ADMET properties of Syzygium aromaticum.

Toxicity prediction was carried out in this study using 43 ligand compounds using admetSAR. This prediction is carried out to evaluate the potential danger of compounds as drug candidates to humans and the environment. The toxicity prediction requirements used in this study are human either a go-go-related gene (hERG), carcinogenic potential, and acute oral toxicity. These three parameters are criteria for identifying potential compounds as anti-inflammatory drugs, one of which is antidiabetic. Of the 43 compounds that have passed the toxicity screening test using admetSAR, only 8 compounds do not meet one of the three toxicity

criteria listed in Table 5. Therefore, the remaining 35 compounds will proceed to the molecular tethering stage.

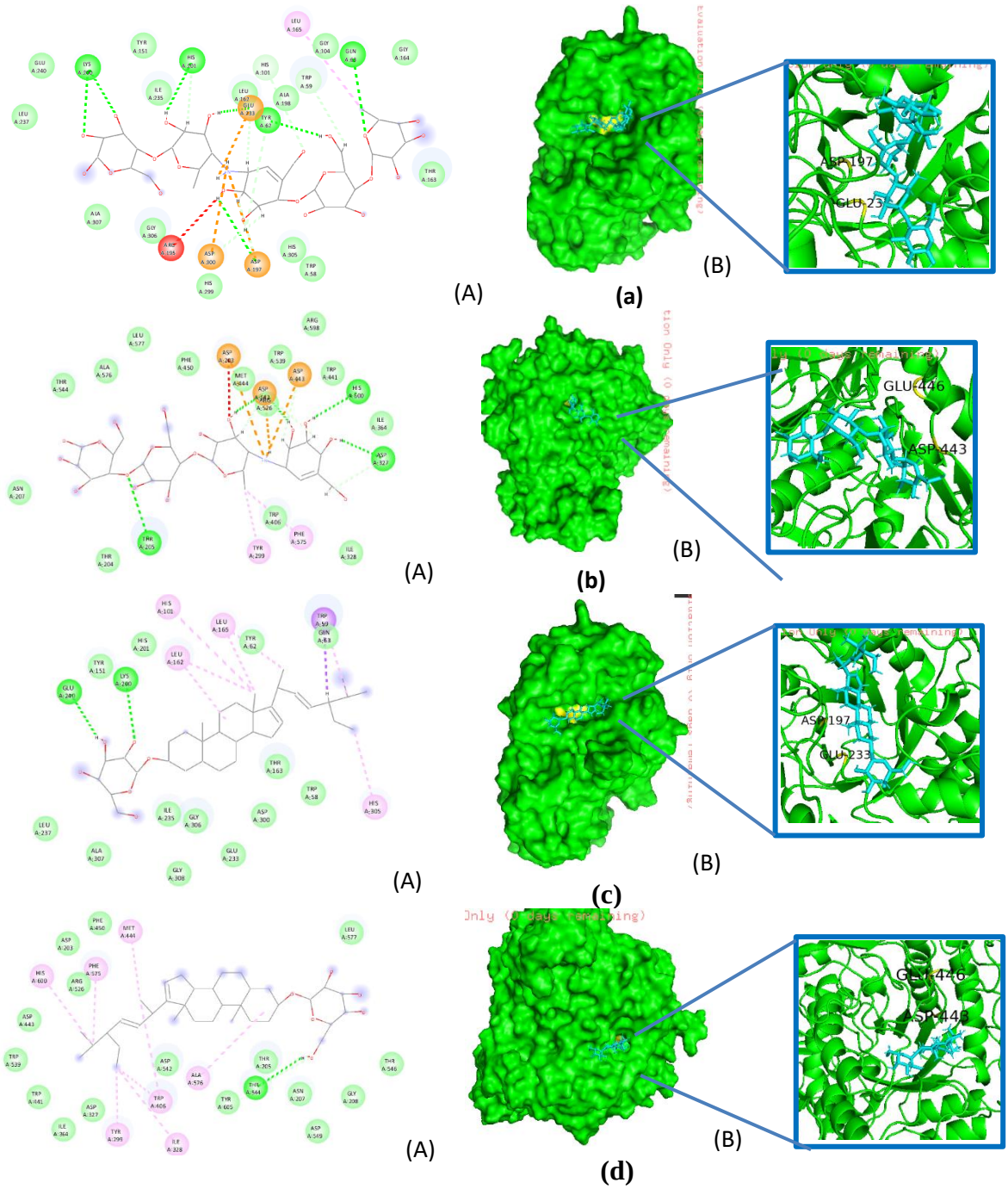

Figure 1. (a) Visualization of Molecular Docking of natural ligands of Acarbose alpha-amylase; **(b)** Visualization of natural ligands of Acarbose Alpha glucosidase; **(c)** Visualization of Stigmaterol alpha-amylase; **(d)** Visualization of Stigmasterol Alpha glucosidase A) 2D diagram of hydrogen bonds and hydrophobic interactions between ligands-receptors; B) Fastening pouch.

Table 5. ADMET toxicity prediction for constituents.

No	Constituents	hERG		Karsinogenitas		Toksisitas oral akut	
		Category	Probability	Category	Probability	Category	Probability
1	Eugenol	Weak inhibitor	0.8355	Non-carcinogens	0.8432	III	0.8605
2	Beta-caryophyllene	Weak inhibitor	0.9225	Non-carcinogens	0.6863	III	0.82
3	Aeruginosin	Weak inhibitor	0.8725	Non-carcinogens	0.5091	III	0.5708
4	Quercetin	Weak inhibitor	0.9781	Non-carcinogens	0.945	II	0.7348
5	Euparin	Weak inhibitor	0.8582	Non-carcinogens	0.9091	III	0.5191
6	L-Noradrenaline	Weak inhibitor	0.9028	Non-carcinogens	0.8942	II	0.4487
7	Benzofuran	Weak inhibitor	0.9324	Non-carcinogens	0.9345	I	0.4444

No	Constituents	hERG		Karsinogenitas		Toksisitas oral akut	
		Category	Probability	Category	Probability	Category	Probability
8	Gallic acid	Weak inhibitor	0.9821	Non-carcinogens	0.9177	III	0.6904
9	Myricetin	Weak inhibitor	0.9781	Non-carcinogens	0.945	II	0.7348
10	2-Heptanone	Weak inhibitor	0.8591	Carcinogens	0.6445	III	0.8291
11	5-Hydroxytryptamine	Weak inhibitor	0.8375	Non-carcinogens	0.9414	II	0.4319
12	Tryptamine	Weak inhibitor	0.9337	Non-carcinogens	0.9255	III	0.4823
13	Biflorin	Weak inhibitor	0.9689	Non-carcinogens	0.9498	III	0.4784
14	Syringic acid	Weak inhibitor	0.9858	Non-carcinogens	0.8809	II	0.4765
15	Vanillin	Weak inhibitor	0.9664	Non-carcinogens	0.8759	III	0.8545
16	Casuarictin	Weak inhibitor	0.9758	Non-carcinogens	0.964	III	0.5277
17	Eugeniin	Weak inhibitor	0.9758	Non-carcinogens	0.964	III	0.5277
18	Tellimagrandin I	Weak inhibitor	0.9775	Non-carcinogens	0.9667	III	0.4838
19	Campesterol	Weak inhibitor	0.773	Non-carcinogens	0.932	I	0.5508
20	Kaempferol	Weak inhibitor	0.9795	Non-carcinogens	0.9363	II	0.6238
21	Rhamnocitrin	Weak inhibitor	0.9766	Non-carcinogens	0.936	III	0.7641
22	Rhamnetin	Weak inhibitor	0.975	Non-carcinogens	0.9449	III	0.6733
23	Isoengeletin	Weak inhibitor	0.9846	Non-carcinogens	0.9461	III	0.5184
24	Ellagic acid	Weak inhibitor	0.9721	Non-carcinogens	0.9582	II	0.602
25	Viscic acid	Weak inhibitor	0.9261	Non-carcinogens	0.9474	III	0.6963
26	Oleanolic acid	Weak inhibitor	0.9582	Non-carcinogens	0.9394	III	0.8316
27	3-O-beta-D-Glucopyranosyl sitosterol	Weak inhibitor	0.9452	Non-carcinogens	0.9587	III	0.6774
28	Stigmasterol-3-O-beta-D-glucopyranoside	Weak inhibitor	0.9452	Non-carcinogens	0.9587	III	0.6774
29	Eugenin	Weak inhibitor	0.9302	Non-carcinogens	0.9209	III	0.7746
30	Isobiflorin	Weak inhibitor	0.9689	Non-carcinogens	0.9498	III	0.4784
31	Methyl salicylate	Weak inhibitor	0.9496	Non-carcinogens	0.8577	III	0.8105
32	Strictinin	Weak inhibitor	0.9775	Non-carcinogens	0.9667	III	0.4838
33	Isoeugenitin	Weak inhibitor	0.9264	Non-carcinogens	0.9158	II	0.5409
34	Isoeugenitol	Weak inhibitor	0.9395	Non-carcinogens	0.9258	III	0.6826
35	m-Methoxybenzaldehyde	Weak inhibitor	0.8824	Non-carcinogens	0.7956	III	0.9029
36	5-Methoxytryptamine	Weak inhibitor	0.7913	Non-carcinogens	0.9555	III	0.5503
37	Melatonin	Weak inhibitor	0.9631	Non-carcinogens	0.9498	III	0.7793
38	Aceteugenol	Weak inhibitor	0.9535	Non-carcinogens	0.8445	III	0.8552
39	2-Acetyl-4-beta-D-glucopyranosyl-1,3,5-benzenetriol.	Weak inhibitor	0.97	Non-carcinogens	0.9362	III	0.6737
40	Syzyginin A	Weak inhibitor	0.9758	Non-carcinogens	0.964	III	0.5277
41	Syzyginin B	Weak inhibitor	0.9775	Non-carcinogens	0.9667	III	0.4838
42	Daucosterol	Weak inhibitor	0.9452	Non-carcinogens	0.9587	III	0.6774
43	Tellimagrandin 2	Weak inhibitor	0.9758	Non-carcinogens	0.964	III	0.5277

Human ether parameters are a go-go-related gene (heRG). The hERG gene parameter acts as a gene that codes for potassium ion channels in regulating repolarization and pore formation in the flow of current to the heart [19]. This role makes this parameter important in determining the potential of a drug candidate because the heRG gene can slow down to stop heart activity so that the ligand pass requirement is a weak inhibitor [20]. Carcinogen parameters in drug candidates indicate the potential for cancer, so the requirements for passing these parameters are non-carcinogenic or weakly carcinogenic with conditions (TD50>10 mg kg 1 per day). The parameters of acute oral toxicity in drug candidates refer to the median lethal dose (LD50) after administration of a single dose of a drug compound within a span of 24 hours with the condition that it passes the test, namely in category III toxic while (500 mg kg^{-1} < LD50, 5000 mg kg^{-1}) and IV are not toxic or safe (5000 mg kg^{-1} < LD50) [21].

3.4. Simulation molecular dynamics.

3.4.1. Structural stability from analysis root mean square deviation (RMSD).

The ligand-to-protein binding mode was considered stable if the Root Mean Square Deviation (RMSDbb) of the protein backbone in the last 5 ns of the simulation was less than 2 Å [17]. All stable ligand complexes produced similar RMSDbb values for the 100 ns simulation. Acarbose docked with α-glucosidase and α-amylase appeared more stable than acarbose, as shown in Figure 2 and Figure 3. The average values of stigmasterol-3-O-beta-D-glucopyranoside and acarbose from the alfa-glucosidase results were 1.355 Å and 1.254 Å, respectively. Stigmasterol-3-O-beta-D-glucopyranoside and acarbose from the results of the alpha-amylase dynamic produce an average RMSD of 1.212 Å and 1.105 Å. The structural stabilization of the complex is demonstrated by a lower RMSD value of ligand–docked protein than solitary one [22].

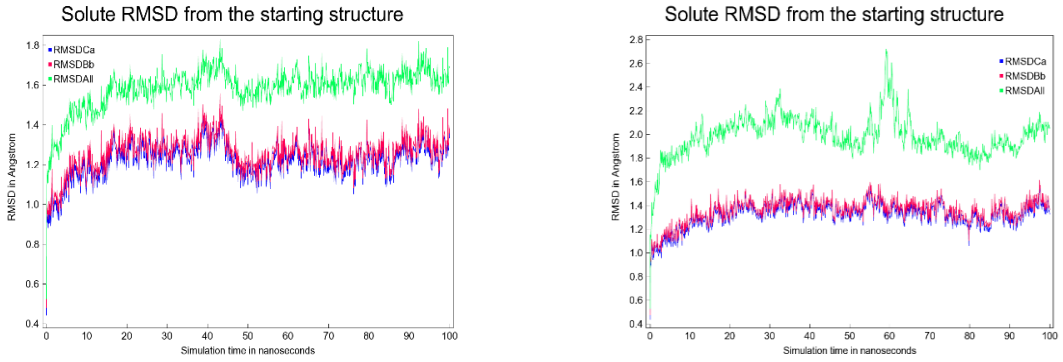

(**a**) (**b**)

Figure 2. Alfa glucosidase; **(a)** Acarbose; **(b)** Stigmasterol-3-O-beta-D-glucopyranoside.

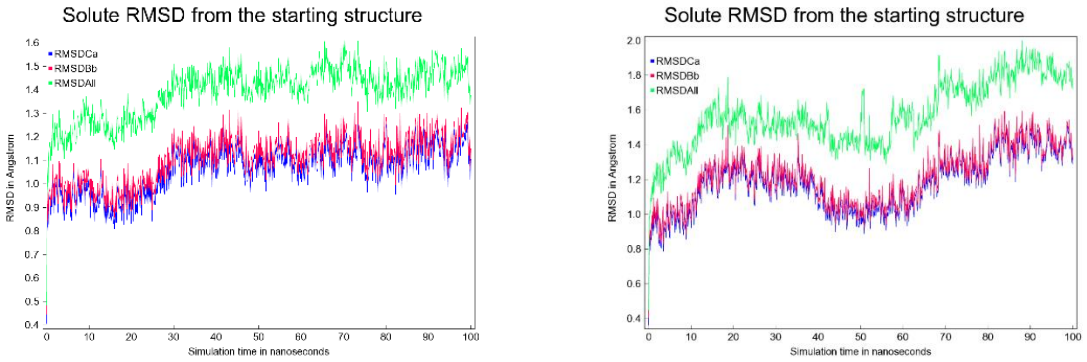

(**a**) (**b**)

Figure 3. Alfa amylase; **(a)** Acarbose; **(b)** Stigmasterol-3-O-beta-D-glucopyranoside.

3.4.2. Fluctuation of the conformation enzymes.

The interaction between the ligand and receptor is usually either attractive or repulsive. The bonded residue underwent a slight shift due to the influence of the ligand. This shift can be seen from the Root Mean Square Fluctuation (RMSF) value during the 50 ns simulation. RMSF shows the stiffness of the residual structure during simulation. Table 2 shows the RMSF results for the four complexes in terms of the residues of the active sites of the α-glucosidase and α-amylase enzymes. All ligand complexes had small RMSF values with respect to the active-site residue. RMSF calculations represent the dynamics of backbone atoms, with higher values indicating greater flexibility [23]. Ligand in which each complex residue has an RMSF value lower than 1.4 Å indicates the stable nature of the protein-peptide [24]. The RMSF

attribute allows certain modifications in the protein chain indicated in the catalytic domain, and RMSF values on the backbone protein can show fluctuations from the N and C terminals [25]. This was also the case for all the tested ligand complexes (Table 6). None of the ligands produced an RMSF value of more than 1.4 Å at the active site, indicating that none have less binding stability. Based on the RMSF values produced on the active sites, x produces the smallest value compared to the acarbose.

Table 6. Root mean square fluctuation of alfa glucosidase and alfa amylase.

Residue	Root Mean Square Fluctuation (Å)			
	Alfa glucosidase		Alfa amylase	
	Stigmasterol-3-O-beta-D-glucopyranoside	Acarbose	Stigmasterol-3-O-beta-D-glucopyranoside	Acarbose
ASP443	0.825	0.563		
GLU446	0.493	0.415		
ASP197			0.719	0.404
GLU233			0.977	0.914

3.4.2.1. Compactness of complex ligand's structure.

The average gyration (Rg) radius of each complex from α-glucosidase was 28.543 Å by stigmasterol-3-O-beta-D-glucopyranoside and 28.465 Å by acarbose (Figure 4). Meanwhile, each complex produced 23.270 Å by stigmasterol-3-O-beta-D-glucopyranoside from alpha-amylase and 23.198 Å by acarbose (Figure 5). Stigmasterol-3-O-beta-D-glucopyranoside from alfa glucosidase and alfa amylase have demonstrated higher values, indicating a loose protein structure packing, which means a more flexible protein conformation [23]. The radius of gyration is considered a fundamental indicator of the total size of chain molecules.

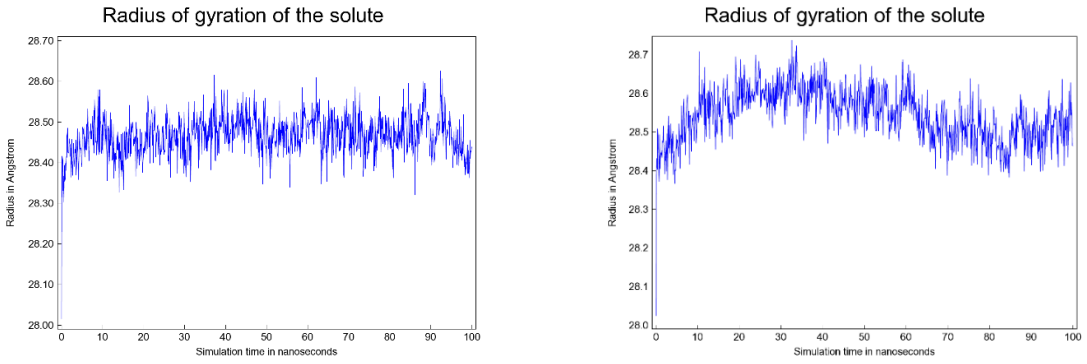

(**a**) (**b**)

Figure 4. Alfa glucosidase; **(a)** Acarbose; **(b)** Stigmasterol.

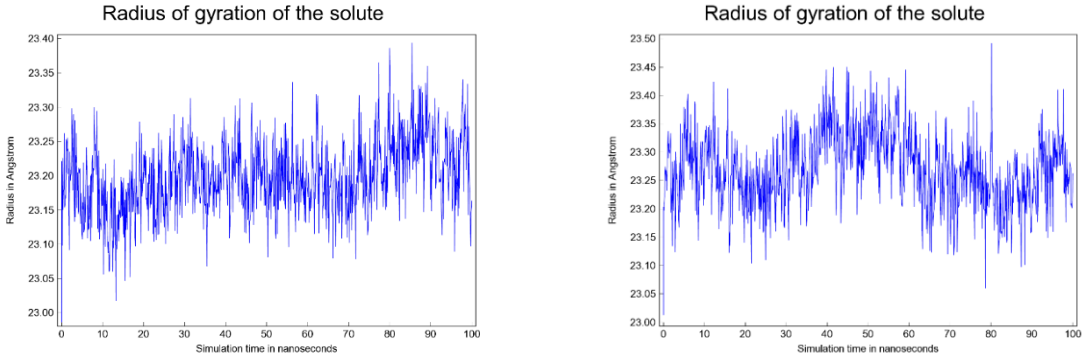

(**a**) (**b**)

Figure 5. Alfa amylase; **(a)** Acarbose; **(b)** Stigmasterol.

Rg evaluates the compactness and flexibility of the protein inside a biological environment to compare the protein structure per unit of time to the hydrodynamic radius, which can be monitored experimentally [22].

3.4.3. Binding free energy calculation analysis.

The molecular mechanics Poisson–Boltzmann Surface Area (MM-PBSA) binding energy results are plotted against a 100 ns simulation for alpha-glucosidase and alpha-amylase, as shown in Figure 6. The average free binding energies of acarbose-alpha glucosidase, stigmasterol-3-O-beta-D-glucopyranoside obtained the best for alfa glucosidase, acarbose-amylase, and stigmasterol-3-O-beta-D-glucopyranoside as the best for alfa amylase are respectively -254903 cal/mol, 2327 cal/mol, -335644 cal/mol, and 27374 cal/mol. YASARA's built-in macros are used to run calculations, where more positive energy indicates better binding [26]. The stigmasterol-3-O-beta-D-glucopyranoside-alpha glucosidase, acarbose-alpha glucosidase, stigmasterol-3-O-beta-D-glucopyranoside-alpha amylase, and acarbose-alpha amylase complexes had 551, 0, 759, and 0 positive bonds, respectively. The MM-PBSA approach addresses the contributions from electrostatic and van der Waals interactions and changes in solvation to binding affinities. In molecular modeling and computational drug design schemes, the PBSA system is a widely used solvation model for estimating the binding free energy of drug-protein complexes [27].

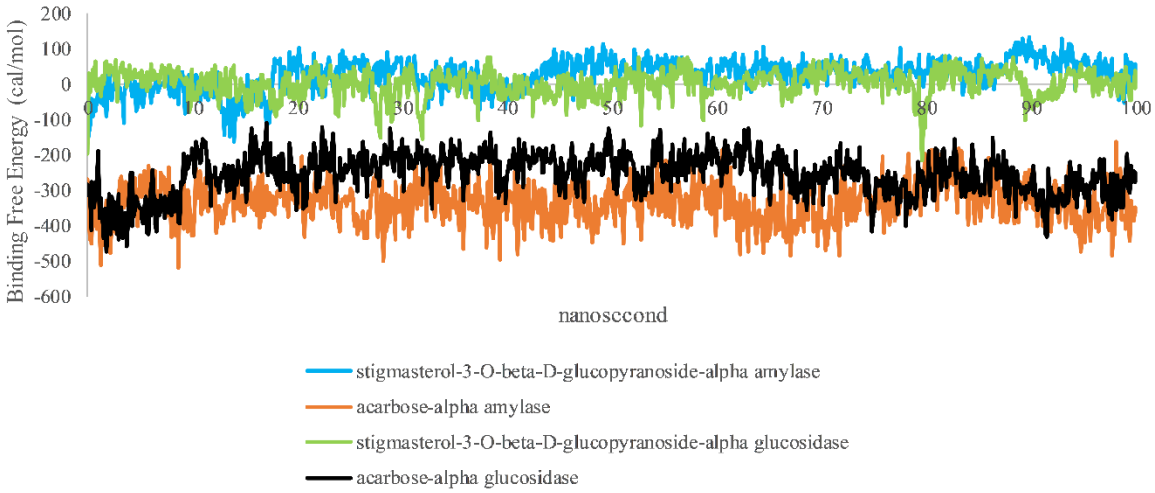

Figure 6. Binding free energy molecular dynamics simulation.

4. Conclusions

The best inhibition of both enzymes is owned by stigmasterol ligands with binding free energy of -9506 cal/mol to alpha-amylase and -8385 cal/mol to alpha-glucosidase. The average free binding energy of stigmasterol-3-O-beta-D-glucopyranoside ligands is better than natural ligands from both alpha-glucosidase and alpha-amylase based on the best results from molecular dynamics simulations with values of 2327 cal/mol and 27374 cal/mol.

Funding

This research received no external funding.

Acknowledgments

Thank you to Gusnia Meilin Gholam from Biomatics.

Conflicts of Interest

The authors declare no conflict of interest

References

1. [WHO] World Health Organization. Available online: Cardiovascular disease (accessed on 25 october **2023**), https://www.who.int/news-room/fact-sheets/detail/cardiovascular-diseases-(cvds).
2. Ngaruiya, C.; Bernstein, R.; Leff, R.; Wallace, L.; Agrawal, P.; Selvam, A.; Hersey, D.; Hayward, A. Systematic review on chronic non-communicable disease in disaster settings. *BMC Public Health* **2022**, *22*, 1234, https://doi.org/10.1186/s12889-022-13399-z.
3. Kohrt, B.A.; Mistry, A.S.; Anand, N.; Beecroft, B.; Nuwayhid, I. Health research in humanitarian crises: an urgent global imperative. *BMJ Global Health* **2019**, *4*, e001870, https://doi.org/10.1136/bmjgh-2019-001870.
4. [IDF] IDF Diabetes Atlas. Available online: URL (accessed on 26 October **2023**), https://www.diabetesatlas.org/data/en/world/.
5. IBRD (International Bank for Reconstuction and Development). Available online: URL (accessed 26 October **2023**), https://www.worldbank.org/in/country/indonesia/overview.
6. Wang, J.; Chu, H.; Li, H.; Yang, W.; Zhao, Y.; Shen, T.; Cary, J.; Zhang, L. A Network Pharmacology Approach to Investigate the Mechanism of Erjing Prescription in Type 2 Diabetes. *Evid. -Based Complementary Altern. Med.* **2021**, *2021*, 9933236, https://doi.org/10.1155/2021/9933236.
7. Schlesinger, S.; Neuenschwander, M.; Barbaresko, J.; Lang, A.; Maalmi, H.; Rathmann, W.; Roden, M.; Herder, C. Prediabetes and risk of mortality, diabetes-related complications and comorbidities: umbrella review of meta-analyses of prospective studies. *Diabetologia* **2022**, *65*, 275–285, https://doi.org/10.1007/s00125-021-05592-3.
8. Clair, C.; Meigs, J.B.; Rigotti, N.A. Smoking Behavior among US Adults with Diabetes or Impaired Fasting Glucose. *Am. J. Med.* **2013**, *126*, 541.e515-541.e518, https://doi.org/10.1016/j.amjmed.2012.11.029.
9. Saras, T. Cengkeh: Keajaiban Herbal dalam Pengobatan dan Kesehatan; Tiram Media, Semarang, **2023**; 1-65.
10. Haro-González, J.N.; Castillo-Herrera, G.A.; Martínez-Velázquez, M.; Espinosa-Andrews, H. Clove Essential Oil (*Syzygium aromaticum* L. Myrtaceae): Extraction, Chemical Composition, Food Applications, and Essential Bioactivity for Human Health. *Molecules* **2021**, *26*, 6387, https://doi.org/10.3390/molecules26216387.
11. Astuti, R.I.; Listyowati, S.; Wahyuni, W.T. Life span extension of model yeast Saccharomyces cerevisiae upon ethanol derived-clover bud extract treatment. *IOP Conf. Ser. Earth Environ. Sci.* **2019**, *299*, 012059, https://doi.org/10.1088/1755-1315/299/1/012059.
12. Ashfani, N.F. Antioxidant and Antimutagenic Activities from Extracellular Metabolites of Clove Endophytic Bacteria Extract (*Syzygium aromaticum* L.), Graduate Thesis, IPB University, Bogor, Indonesia, **28 November 2022**.
13. Shinbo, Y.; Nakamura, Y.; Altaf-Ul-Amin, M.; Asahi, H.; Kurokawa, K.; Arita, M.; Saito, K.; Ohta, D.; Shibata, D.; Kanaya, S. Available online: KNApSAcK: a comprehensive species-metabolite relationship database, *http://www.knapsackfamily.com/KNApSAcK/*.
14. [IJAH IPB]. Kusuma, W.A.; Wijaya, S.H.; Heryanto, R. Available online: Indonesia Jamu-Herbs (IJAH), https://ijah.apps.cs.ipb.ac.id/#/home.
15. Riyan Alifbi Putera, I.; Djarot Sasongko Hami, S.; Mega, S.; Rini, K. PENAPISAN VIRTUAL SENYAWA AKTIF SIRIH MERAH (Piper Crocatum) SEBAGAI INHIBITOR ANGIOTENSIN CONVERTING ENZYME. *Jurnal Farmamedika* **2022**, *7*, 104-113, https://doi.org/10.47219/ath.v7i2.157.
16. Umar, M.; Safithri, M.; Pratama, R. In Silico Study of Anticancer Activity of Red Betel Leaves Bioactive Compounds against Colon Cancer Marker Proteins. *HAYATI J. Biosci.* **2023**, *30*, 113-121, https://doi.org/10.4308/hjb.30.1.113-121.

17. Chairunisa, F.; Safithri, M.; Andrianto, D.; Kurniasih, R.; Irsal, R.A.P. Molecular docking of red betel leaf bioactive compounds (Piper crocatum) as lipoxygenase inhibitor. *Indonesian J. Pharm. Sci. Technol.* **2023**, *10*, 90-103, http://dx.doi.org/10.24198/ijpst.v10i2.38934.
18. Ramírez, D.; Caballero, J. Is It Reliable to Take the Molecular Docking Top Scoring Position as the Best Solution without Considering Available Structural Data?. *Molecules* **2018**, *23*, 1038, https://doi.org/10.3390/molecules23051038.
19. Dulsat, J.; López-Nieto, B.; Estrada-Tejedor, R.; Borrell, J.I. Evaluation of Free Online ADMET Tools for Academic or Small Biotech Environments. *Molecules* **2023**, *28*, 776, https://doi.org/10.3390/molecules28020776.
20. Jing, Y.; Easter, A.; Peters, D.; Kim, N.; Enyedy, I.J. *In Silico* Prediction of hERG Inhibition. *Future Med. Chem.* **2015**, *7*, 571-586, https://doi.org/10.4155/fmc.15.18.
21. Guan, L.; Yang, H.; Cai, Y.; Sun, L.; Di, P.; Li, W.; Liu, G.; Tang, Y. ADMET-score – a comprehensive scoring function for evaluation of chemical drug-likeness. *Med. Chem. Comm.* **2018**, *10*, 148-157, https://doi.org/10.1039/c8md00472b.
22. Ghahremanian, S.; Rashidi, M.M.; Raeisi, K.; Toghraie, D. Molecular dynamics simulation approach for discovering potential inhibitors against SARS-CoV-2: A structural review. *J. Mol. Liq.* **2022**, *354*, 118901, https://doi.org/10.1016/j.molliq.2022.118901.
23. Dash, R.; Ali, M.C.; Dash, N.; Azad, M.A.K.; Hosen, S.M.Z.; Hannan, M.A.; Moon, I.S. Structural and Dynamic Characterizations Highlight the Deleterious Role of SULT1A1 R213H Polymorphism in Substrate Binding. *Int. J. Mol. Sci.* **2019**, *20*, 6256, https://doi.org/10.3390/ijms20246256.
24. Biswas, S.; Mahmud, S.; Mita, M.A.; Afrose, S.; Hasan, M.R.; Shimu, M.S.S.; Saleh, M.A.; Mostafa-Hedeab, G.; Alqarni, A.; Obaidullah, A.J.; *et al.* Molecular docking and dynamics studies to explore effective inhibitory peptides against the spike receptor binding domain of SARS-CoV-2. *Front. Mol. Biosci.* 2022, *8*, 1-11, https://doi.org/10.3389/fmolb.2021.791642.
25. Gopinath, P.; Kathiravan, M.K. Docking studies and molecular dynamics simulation of triazole benzene sulfonamide derivatives with human carbonic anhydrase IX inhibition activity. *RSC Adv* **2021**, *11*, 38079-38093, https://doi.org/10.1039/D1RA07377J.
26. Mitra, S.; Dash, R. Structural dynamics and quantum mechanical aspects of shikonin derivatives as CREBBP bromodomain inhibitors. *J. Mol. Graphics Modell.* **2018**, *83*, 42–52, https://doi.org/10.1016/j.jmgm.2018.04.014.
27. Wang, C.; Nguyen, P.H.; Pham, K.; Huynh, D.; Le, T.-B.N.; Wang, H.; Ren, P.; Luo, R. Calculating protein–ligand binding affinities with MMPBSA: Method and error analysis. *J. Comput. Chem.* **2016**, *37*, 2436-2446, https://doi.org/10.1002/jcc.24467.